Supporting Information

Significantly Enhanced Oxygen Reduction Reaction Performance of N-doped Carbon by Heterogeneous Sulfur Incorporation: Synergistic Effect Between the two Dopants in Metal-free Catalysts

Jianbing Zhu[a,b], Kai Li[c] Meiling Xiao[a,b], Changpeng Liu[d], Zhijian Wu[c], Junjie Ge[d]* and Wei Xing[a,c,]*

[a]State Key Laboratory of Electroanalytical Chemistry, Changchun Institute of Applied Chemistry, Chinese Academy of Sciences, Changchun, Jilin, 130022, China.

[b]Graduate School of the Chinese Academy of Sciences, Beijing, 100039, China.

[c]State Key Laboratory of Rare Earth Resource Utilization, Changchun Institute of Applied Chemistry, 5625 Renmin Street, Changchun, 130022, PR China.

[d]Laboratory of Advanced Power Sources, Changchun Institute of Applied Chemistry, 5625 Renmin Street, Changchun, 130022, PR China.

Address: 5625 Renmin Street, Changchun 130022, PR China.

E-mail Address: xingwei@ciac.ac.cn

Tel: +86-431-85262223

Fax: +86-431-85685653

Experiment Section

Chemicals

Sulfocarbamide and urea were purchased from Aladdin Company. Black Pearls ® 2000 carbon black was obtained from Cabot Corporation. 5 wt% Nafion ionomer was obtained from Aldrich. Perchloric acid was purchased from Alfa Aesar. Commercial state-of-the-art 20 wt% Pt/C (Johnson Matthey Company, HiSPEC™ 3000) was used as the benchmark for comparison and was denoted as Pt/C. H_2SO_4, $NaNO_3$ and $KMnO_4$ were purchased from the Shanghai Chemical Factory (Shanghai, China) and used as received without further purification. Ultrapure water (Millipore, 18.2 MΩ cm) was used throughout all experiments.

Electrochemical Measurements

RRDE measurements were conducted by liner sweep voltammetry (LSV) from 1.1 V to 0.2 V at a scan rate of 5 mV s^{-1} at 1600 rpm, while the ring electrode was held at 1.3 V vs. RHE. All the ORR currents presented in the figures are Faradaic currents, i.e. after correction for the capacitive current. The following equations were used to calculate n (the apparent number of electrons transferred during ORR) and % H_2O_2 (the percentage of H_2O_2 released during ORR).

$$n = \frac{4I_D}{I_D + (I_R/N)} \qquad (1)$$

$$\%H_2O_2 = 100\,\frac{2I_R/N}{I_D + (I_R/N)} \qquad (2)$$

Where I_D is the Faradaic current at the disk, I_R the Faradaic current at the ring and N is

the H_2O_2 collection coefficient at the ring. The kinetic current (I_k) can be calculated by the Koutechy-Levich equation given blow:

$$\frac{1}{I}=\frac{1}{I_L}+\frac{1}{I_K} \qquad (3)$$

The I_L term can be obtained from the Levich equation:

$$I_L = 0.62nAFC_0(D_0)^{2/3}\nu^{-\frac{1}{6}} \qquad (4)$$

where n is the number of electrons transferred; F is Faraday's constant(96,485 C mol^{-1}); A is the area of the electrode (0:196 cm^2); D is the diffusion coefficient of O_2 in 0.1 M KOH solution (1.9×10^{-5} cm^2 s^{-1}); $\nu$is the kinematic viscosity of the electrolyte (1.01×10^{-2} cm^2 s^{-1}); ω is the angular frequency of rotation, ω = 2πf/60, f is the RDE rotation rate in rpm, and C_0 is the concentration of molecular oxygen in 0.1M KOH solution(1.26×10^{-6} mol cm^{-3}). In all figures, the potentials were converted to values versus the reversible hydrogen electrode (RHE). The conversion from SCE to RHE is done by measuring the voltage ΔE between the SCE and a Pt-black coated Pt wire immersed in the same electrolyte saturated with H_2. The measured ΔE was 0.998 V. All experiments were carried out at about 25°C.

Computational Details

Model

For N doped structure, a 4×4 graphene surface with a single point defect and a benzal N atom (including 31 C and 1 N atoms) are set as the planar unit cell (9.84˚A×9.84˚A× 12˚A) for periodic calculations in this work. For N, S co-doped carbon, the second neighbor C near the defect in N doped structure is replaced by S. The structures of N doped and N, S co-doped are shown in Figure 4a and b, respectively. The geometries are fully optimized after the molecular (O_2, OOH, H_2O

or OH) and O or H atom adsorbed and the most stable structures are shown in Figure S2 (for N doped) and S3 (for N, S co-doped).

The detail about the free energy calculation

To investigate the effects of the electric potential on the activity and mechanisms of ORR, the free energy diagrams of ORR developed by Nørskov et al is employed[1]. Free energy change from initial states to final states of the reaction is calculated as follows:

$$\Delta G = \Delta E + \Delta ZEP - T\Delta S + \Delta G_U + \Delta G_{pH} + \Delta G_{field}$$

where ΔE is the total energy change obtained from DFT calculations, ΔZEP is the change in zero-point energy, T is the temperature (298.15 K), and the ΔS is the change in entropy. $\Delta G_U = -eU$, where U is the electrode potential with respect to standard hydrogen electrode, and e is the transferred charge. $\Delta G_{pH} = k_B T \ln 10 \times pH$ where k_B is the Boltzmann constant, and pH=14 for alkaline medium.[2, 3] ΔG_{field} is the free energy correction due to the electrochemical double layer and is neglected as in previous studies.[1, 4] Gas-phase H_2O at 0.035 bar was used as the reference state, since at this pressure, the gas-phase H_2O is in equilibrium with liquid water at 298.15 K. The entropies of the ORR intermediates were calculated from the vibrational frequencies.

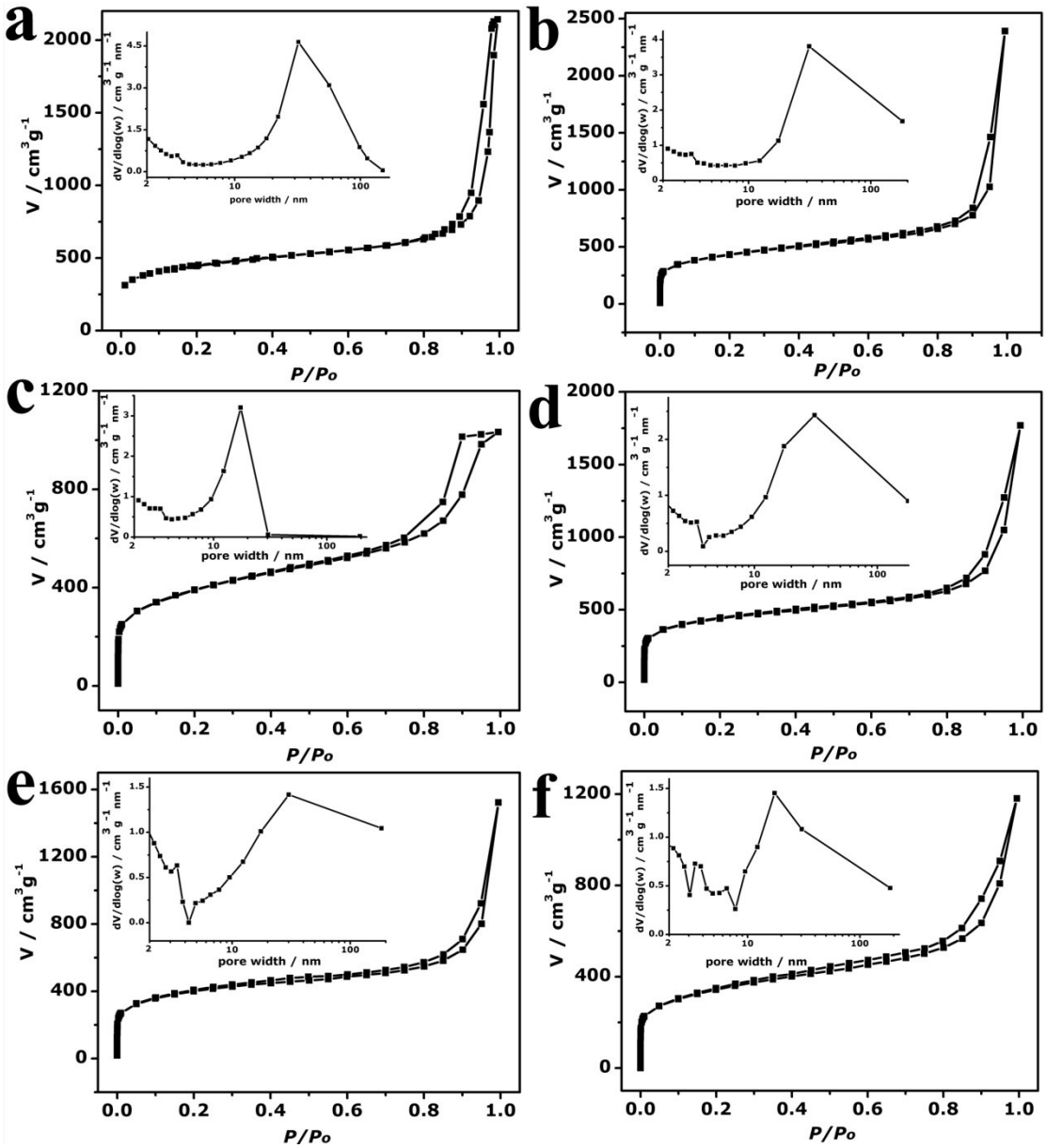

Figure S1 Desorption isotherms of sample obtained with different condition, insert the corresponding pore size distribution curves calculated from the desorption branches; (a) BP, (b) BP-900, (c) OBP-900, (d) N,S-BP-30, (e) N-OBP-30, (f) N,S-OBP-30.

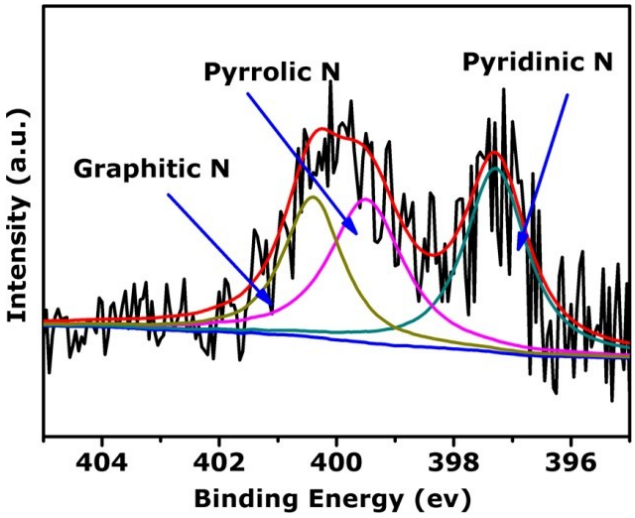

Figure S2 High resolution XPS spectra of N 1s of N-OBP-30.

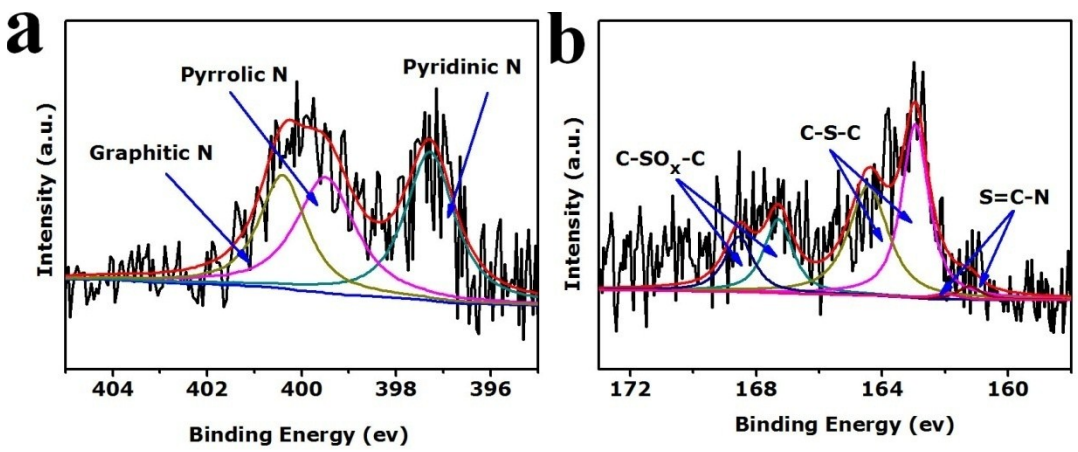

Figure S3 High resolution XPS spectra of N 1s (a) and S 2p (b) of N,S-BP-30.

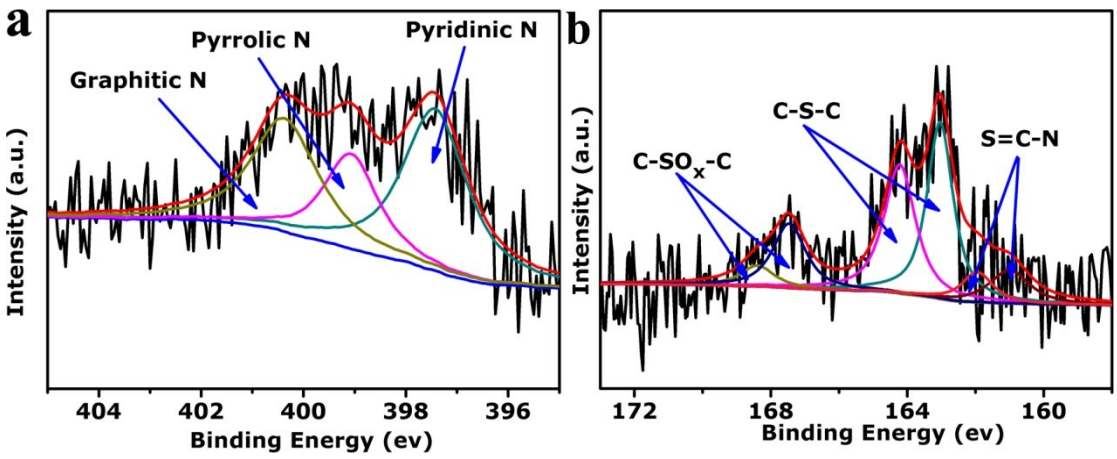

Figure S4 High resolution XPS spectra of N 1s (a) and S 2p (b) of N,S-OBP-30.

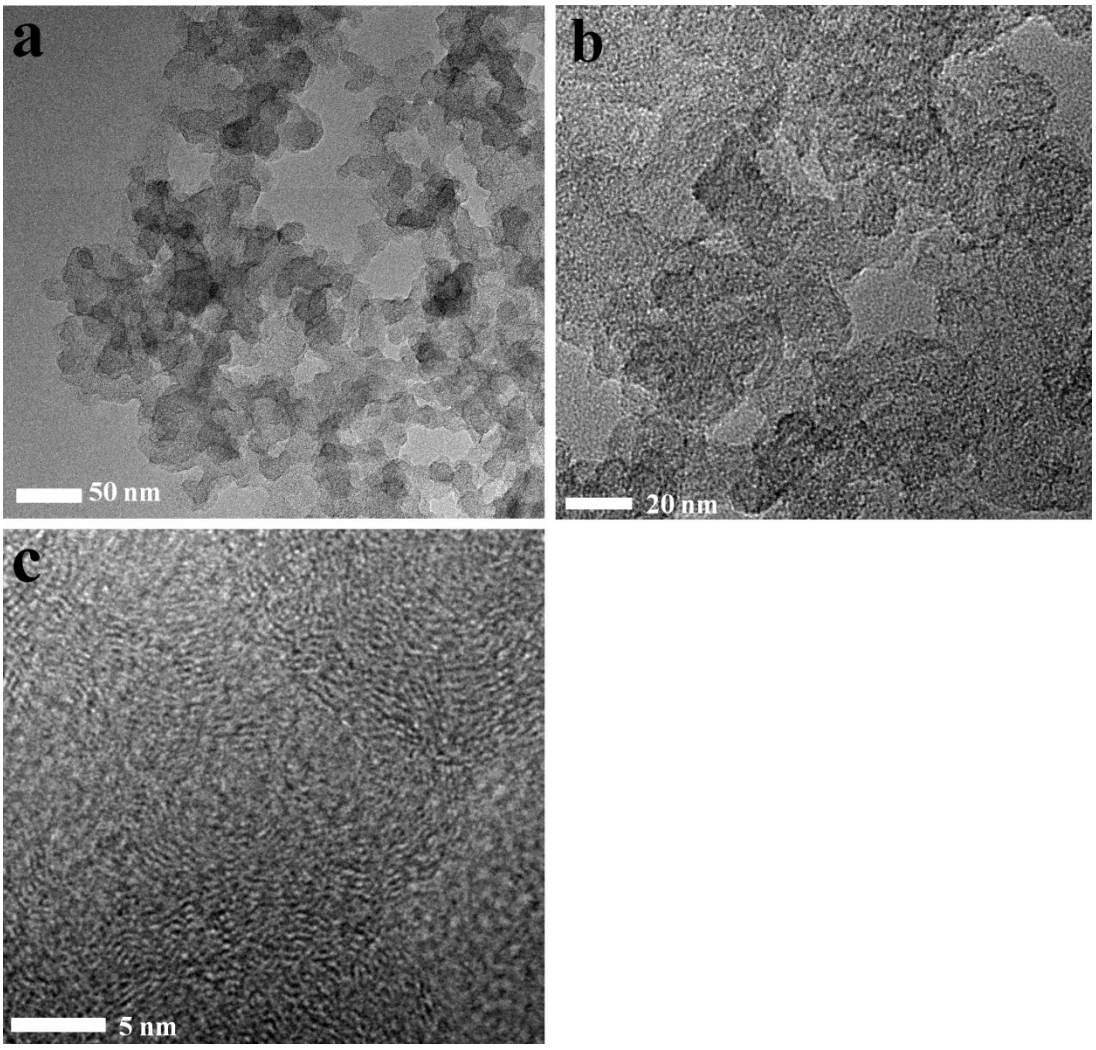

Figure S5 Typical TEM images for OBP-900 with different magnification.

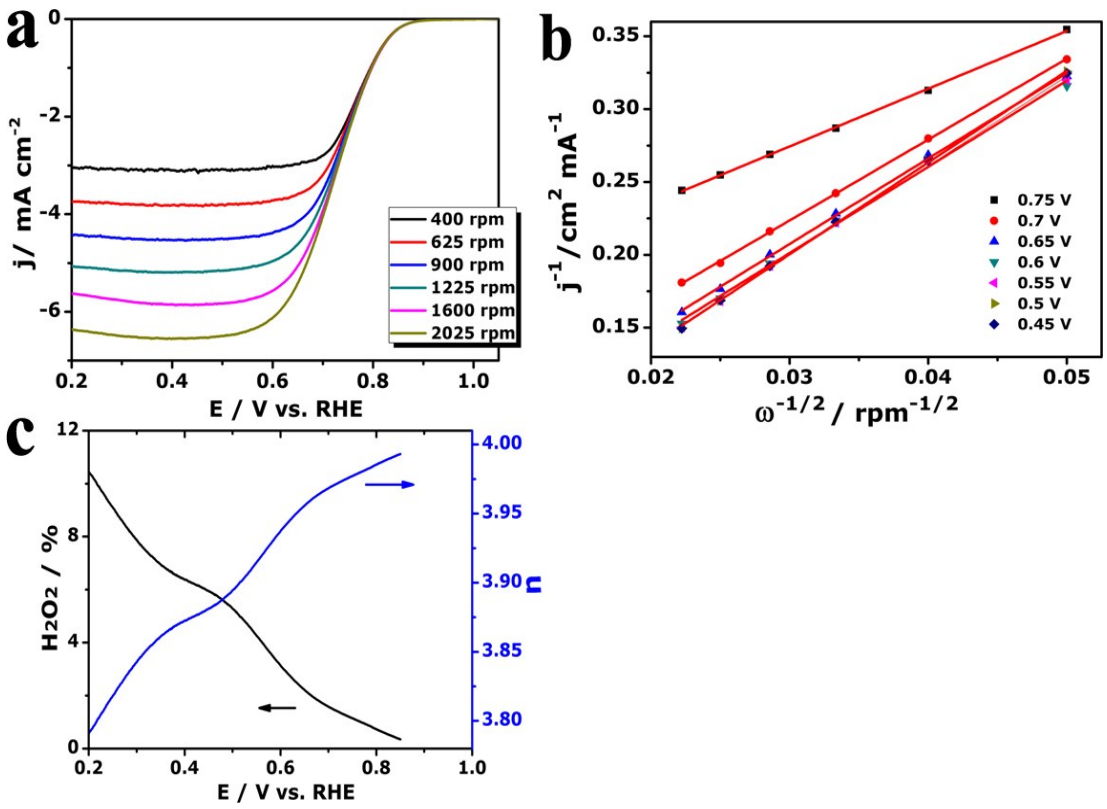

Figure S6 (a) Linear sweep voltammograms (LSV) for oxygen reduction on the N,S-BP-30 catalyst in O_2-saturated 0.1 M KOH at various rotation speeds with a scan rate of 5 mV/s. (b) Corresponding Koutecky–Levich (K-L) plots, (c) peroxide yield and corresponding electron transfer number of N,S-BP-30.

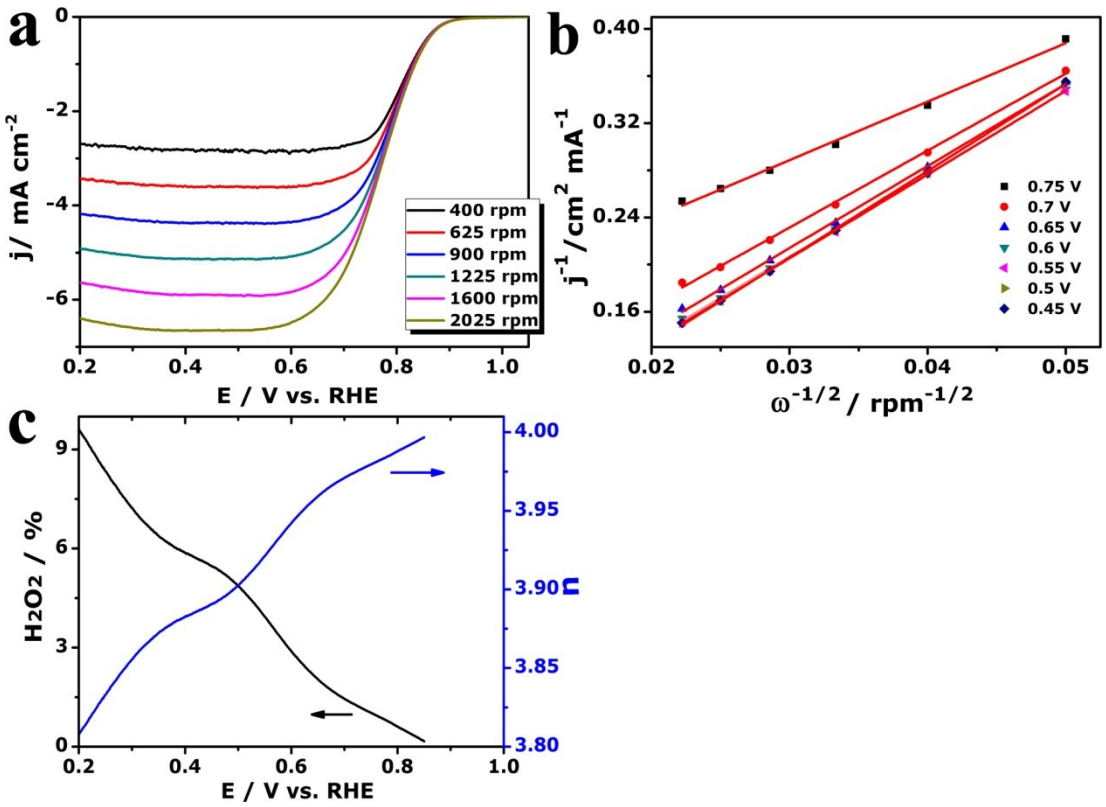

Figure S7 (a) Linear sweep voltammograms (LSV) for oxygen reduction on the N-OBP-30 catalyst in O_2-saturated 0.1 M KOH at various rotation speeds with a scan rate of 5 mV/s. (b) Corresponding Koutecky–Levich (K-L) plots, (c) peroxide yield and corresponding electron transfer number of N-OBP-30.

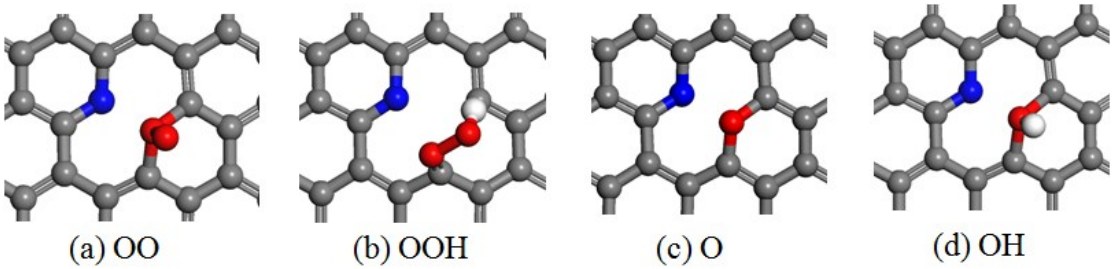

Figure S8 The stable structures of intermediates involved in ORR adsorption on N doped carbon structure. The red and white balls denote the O and H atoms, respectively.

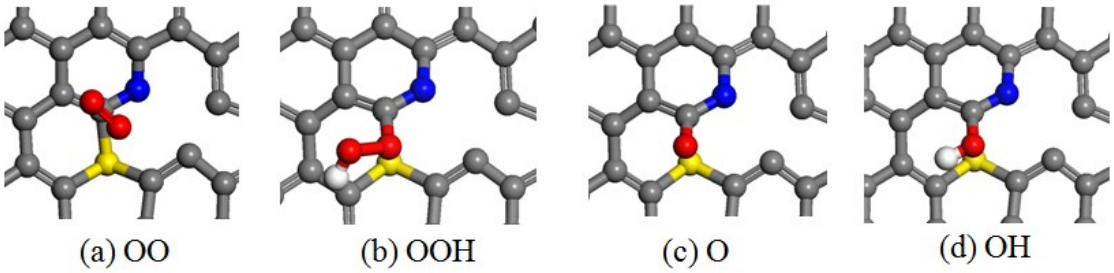

Figure S9 The stable structures of intermediates involved in ORR adsorption on N, S co-doped carbon structure.

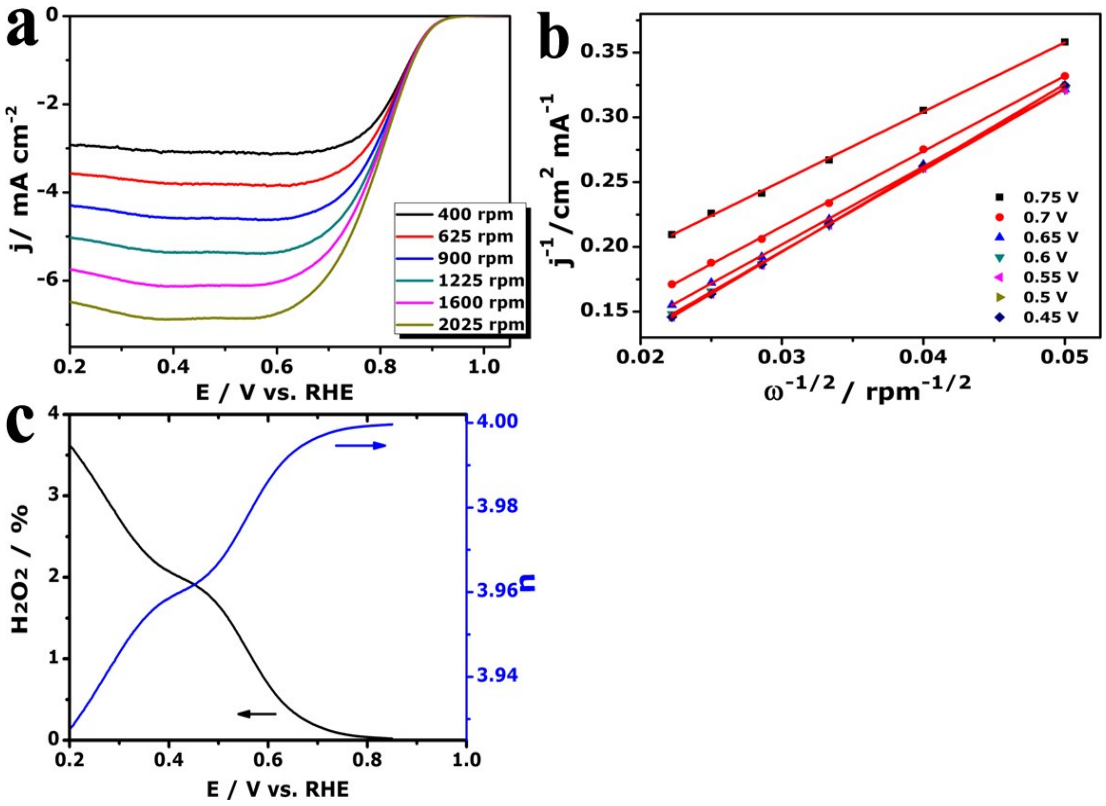

Figure S10 (a) Linear sweep voltammograms (LSV) for oxygen reduction on the N,S-OBP-10 catalyst in O_2-saturated 0.1 M KOH at various rotation speeds with a scan rate of 5 mV/s. (b) Corresponding Koutecky–Levich (K-L) plots, (c) peroxide yield and corresponding electron transfer number of N,S-OBP-10.

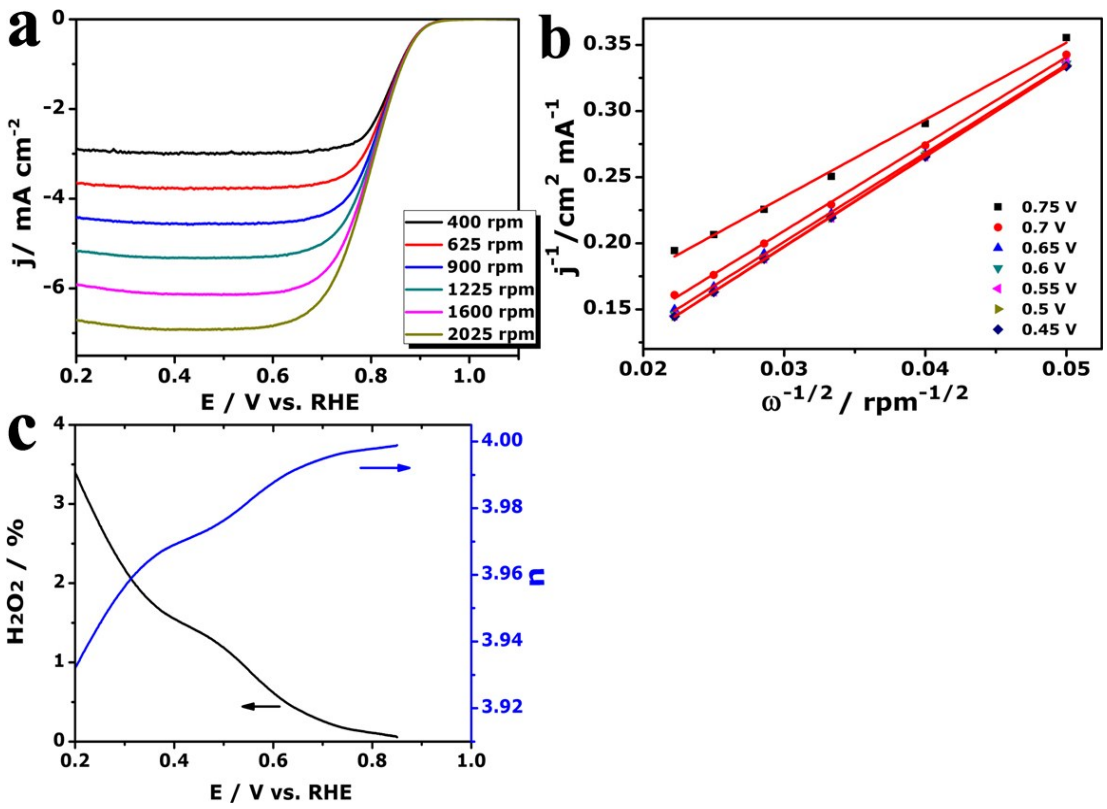

Figure S11 (a) Linear sweep voltammograms (LSV) for oxygen reduction on the N,S-OBP-20 catalyst in O_2-saturated 0.1 M KOH at various rotation speeds with a scan rate of 5 mV/s. (b) Corresponding Koutecky–Levich (K-L) plots, (c) peroxide yield and corresponding electron transfer number of N,S-OBP-20.

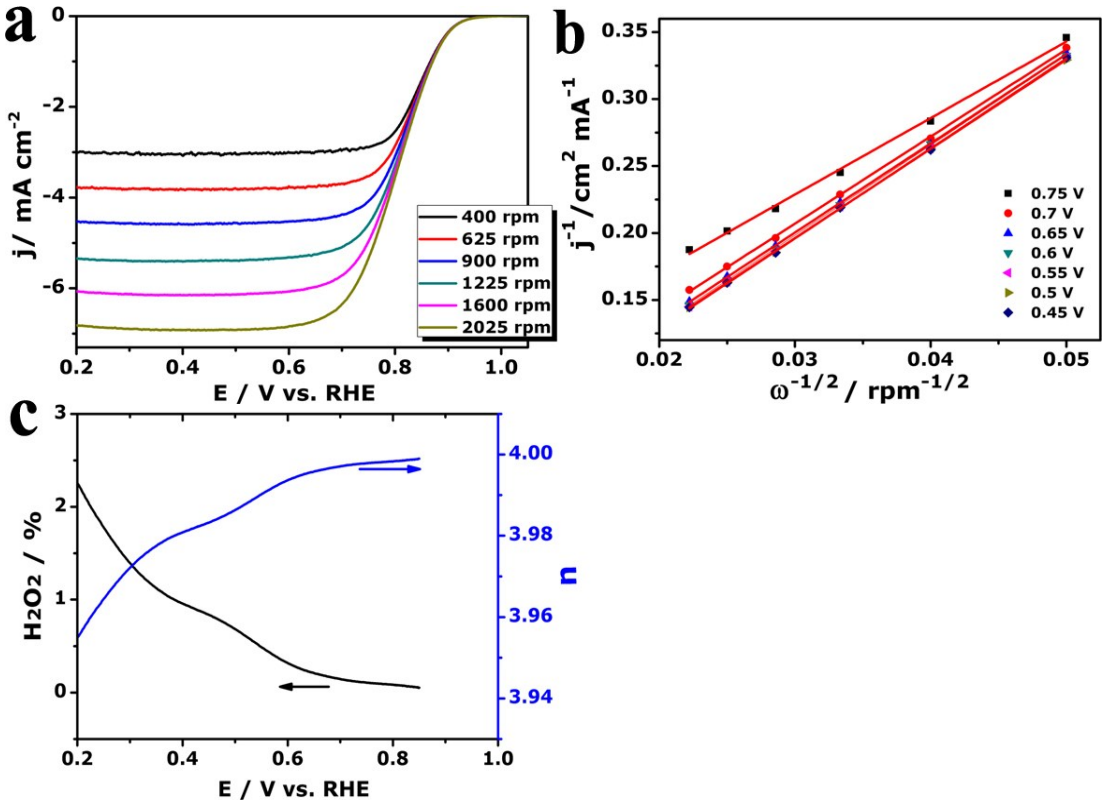

Figure S12 (a) Linear sweep voltammograms (LSV) for oxygen reduction on the N,S-OBP-40 catalyst in O_2-saturated 0.1 M KOH at various rotation speeds with a scan rate of 5 mV/s. (b) Corresponding Koutecky–Levich (K-L) plots, (c) peroxide yield and corresponding electron transfer number of N,S-OBP-40.

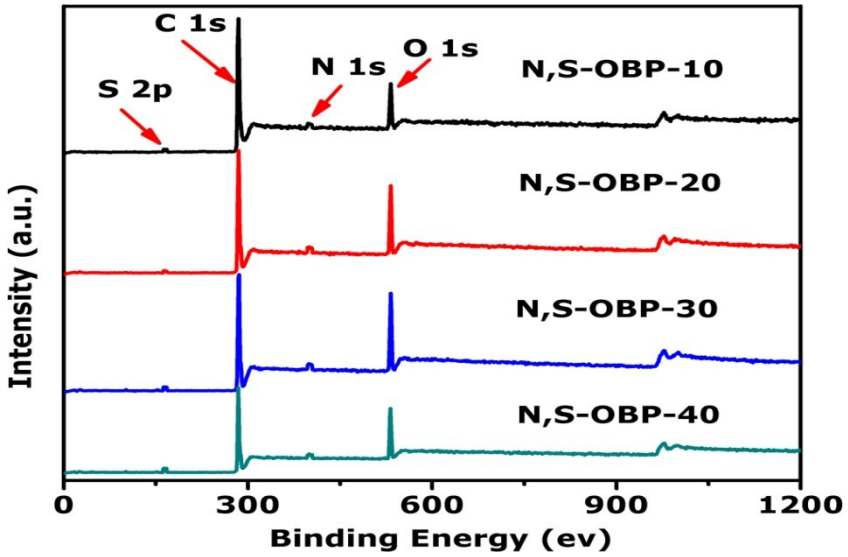

Figure S13 XPS survey spectra of N,S-OBP materials synthesized with different sulfourea/OBP ratio.

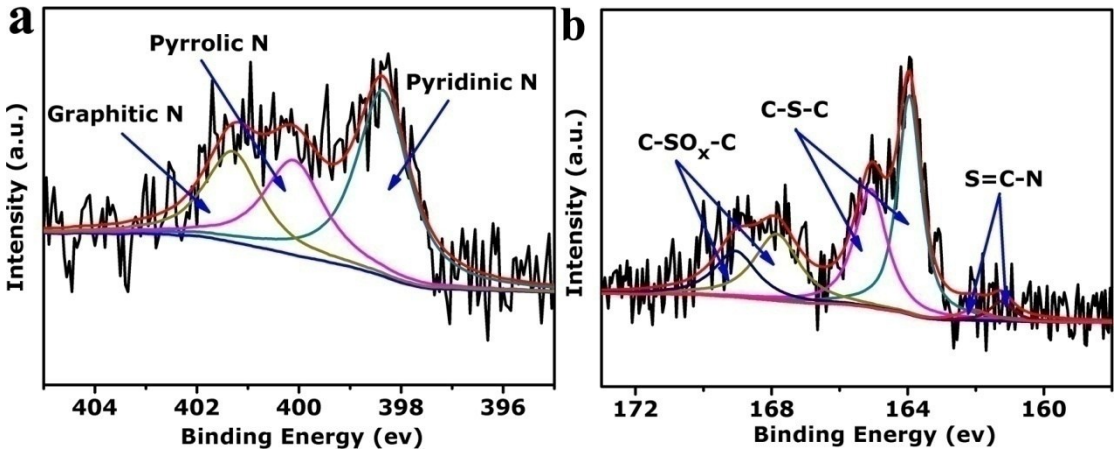

Figure S14 High resolution XPS spectra of N 1s (a) and S 2p (b) of N,S-OBP-10.

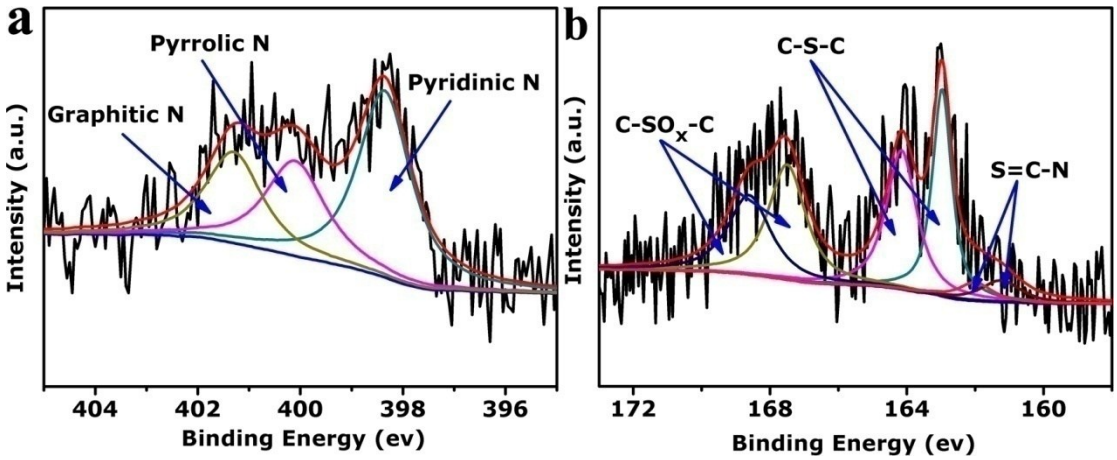

Figure S15 High resolution XPS spectra of N 1s (a) and S 2p (b) of N,S-OBP-20.

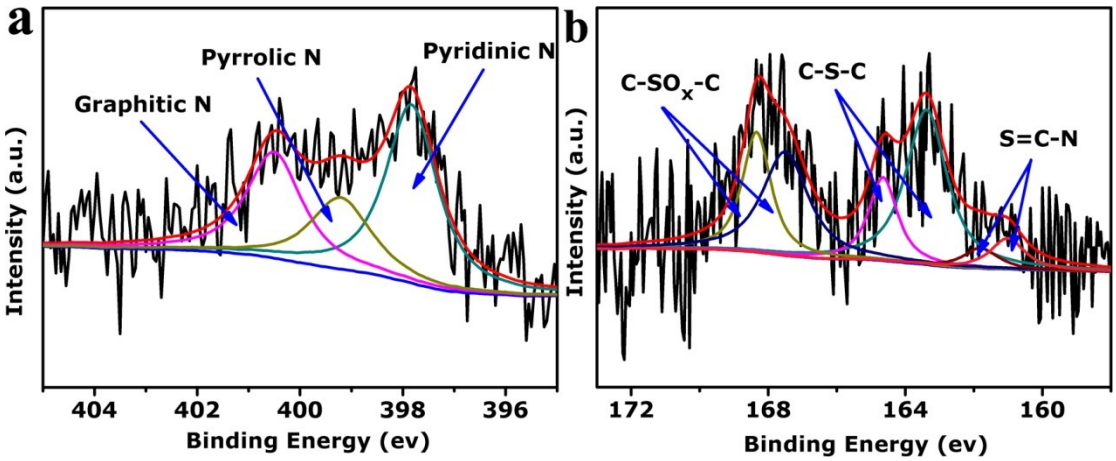

Figure S16 High resolution XPS spectra of N 1s (a) and S 2p (b) of N, S-OBP-40.

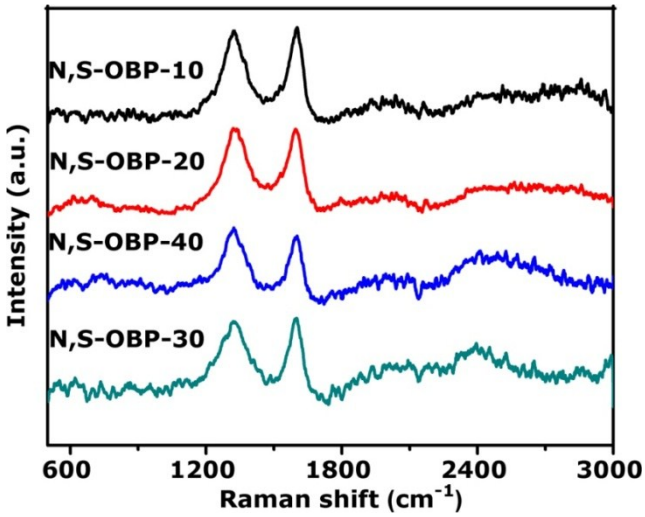

Figure S17 Raman spectra of N,S-OBP materials synthesized with different sulfourea/OBP ratio.

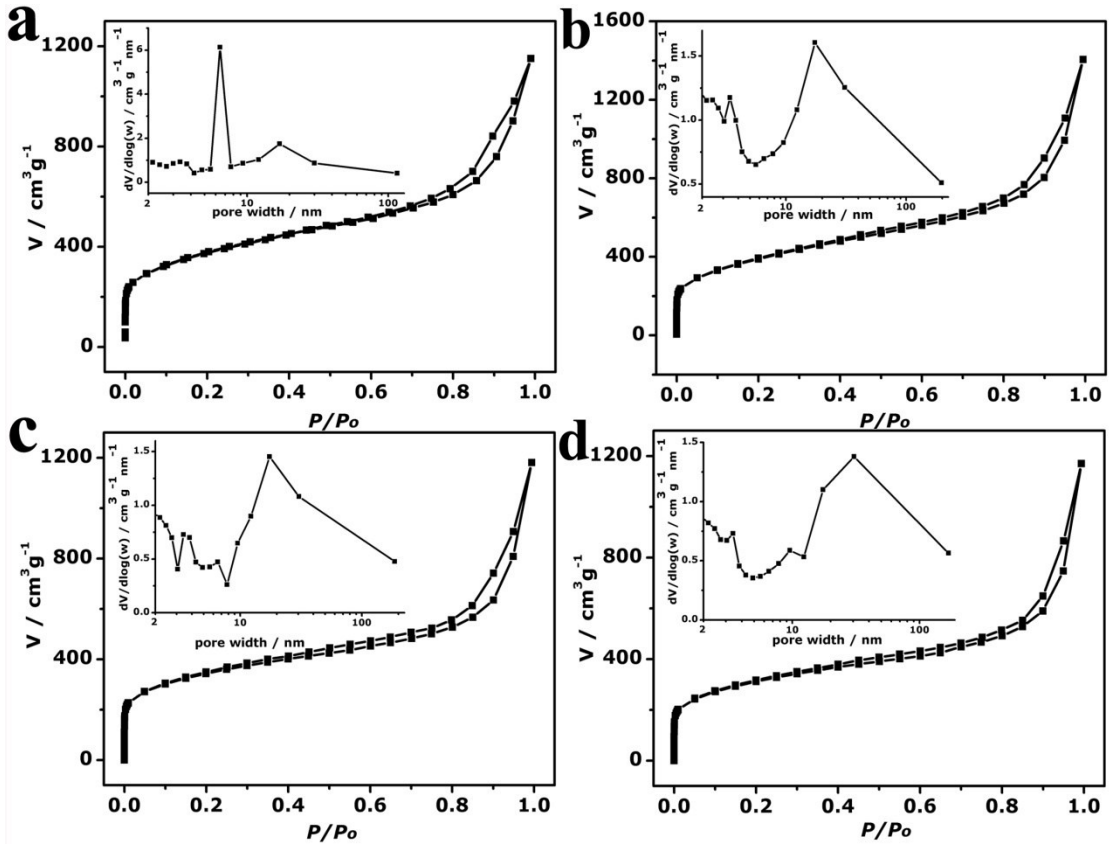

Figure S18 Desorption isotherms of N,S-OBP materials synthesized with differet sulfourea/OBP ratio, insert the corresponding pore size distribution curves calculated from the desorption branches; (a) N,S-OBP-10, (b) N,S-OBP-20, (c) N,S-OBP-30, (d) N,S-OBP-30.

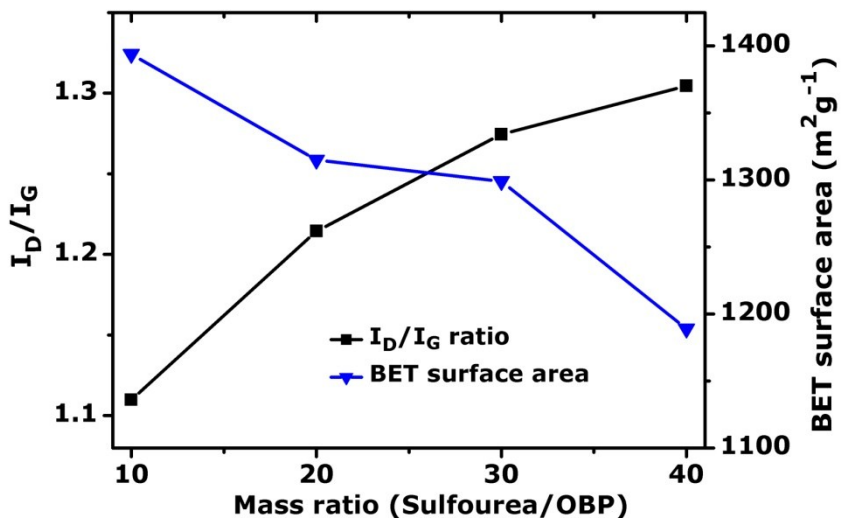

Figure S19 Comparison of I_D/I_G ratio and BET surface area among N, S-OBP-X materials as a function of the sulfourea/OBP ratio.

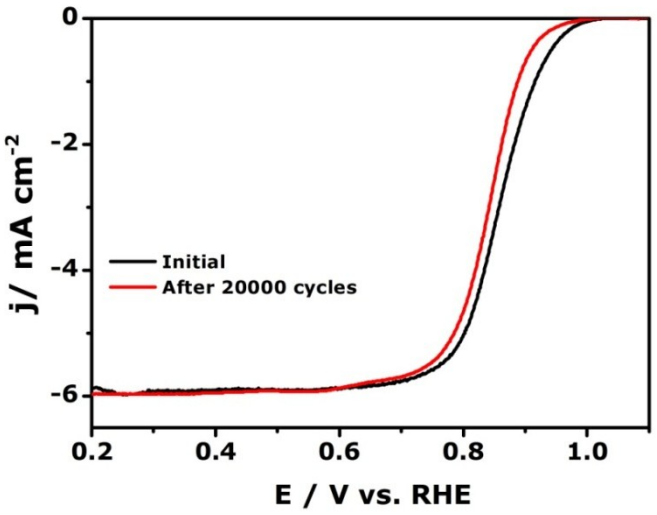

Figure S20 RDE polarization curves for oxygen reduction on Pt/C catalyst at 1600 rpm in O_2-saturated 0.1 M KOH at scan rate of 5 mV s^{-1} before and after 20,000 cycles test.

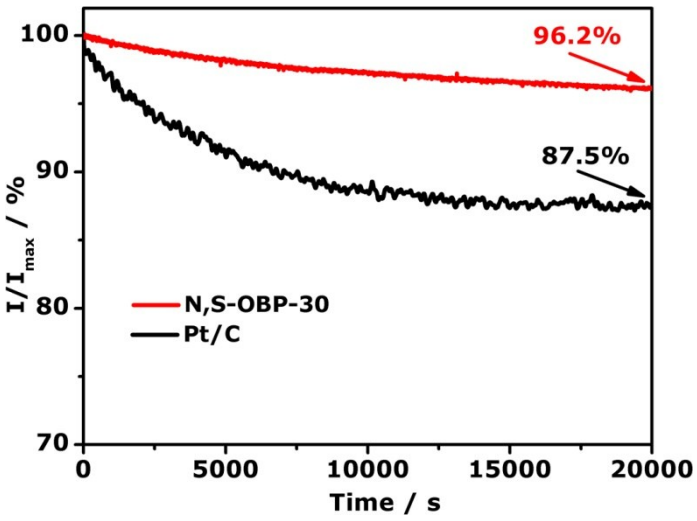

Figure S21 Chronoamperometric measurement of N,S-OBP-30 and Pt/C catalysts at 1600 rpm in O_2-saturated solution 0.1 M KOH, the potential is held at 0.8V.

Table S1 The element composition for the synthesized catalysts

Sample	atomic content / %					
	C[a]	O[a]	N[a]	S[a]	N[b]	S[b]
BP-900	96.68	3.32	NA	NA	0.21	0.22
OBP-900	95.84	4.12	NA	NA	0.25	0.21
N, S-BP-30	91.58	6.5	1.13	0.79	1.30	0.93
N-OBP-30	92.3	5.07	2.63	NA	2.94	0.21
N,S-OBP-30	88.81	5.69	3.82	1.68	4.13	1.98
N,S-OBP-10	91.07	5.71	3.22	1.18	3.39	1.36
N,S-OBP-20	90.13	6.46	3.31	1.31	3.52	1.46
N,S-OBP-40	86.85	6.31	4.67	2.17	5.28	2.41

[a] From XPS result; [b] from elemental analyses

Table S2 BET surfaces area, BJH adsorption main pore size and pore volume for catalysts synthesized at different conditions.

Samples	BET surfaces area / $m^2 g^{-1}$	Pore size / nm	Pore Volume / $cm^3 g^{-1}$
BP-900	1529	31.7	3.700
OBP-900	1374	17.4	1.598
N, S-BP-30	1575	31.1	2.737
N-OBP-30	1427	30.3	2.356
N,S-OBP-30	1212	17.3	1.827
N,S-OBP-10	1394	6.4	1.781
N,S-OBP-20	1315	17.5	2.174
N,S-OBP-40	1189	30.8	1.810

Table S3 The content and type of nitrogen and sulfur of the synthesized samples

Sample	atomic content / %							
	Total N	pyridinic N	pyrrolic N	graphitic N	Total S	C-SOx-C	C-S-C	S=C-N
N, S-BP-30	1.13	0.426	0.5330.	0.209	0.79	0.222	0.540	0.028
N-OBP-30	2.63	1.034	0.534	1.062	-	-	-	-
N,S-OBP-30	3.82	1.724	0.649	1.347	1.68	0.344	1.057	0.279
N,S-OBP-10	3.22	1.542	0.990	0.688	1.18	0.398	0.719	0.063
N,S-OBP-20	3.31	1.549	0.716	1.045	1.31	0.576	0.621	0.113
N,S-OBP-40	4.67	2.134	1.043	1.414	2.17	0.594	1.01	0.203

Reference

1. J. K. Nørskov, J. Rossmeisl, A. Logadottir, L. Lindqvist, J. R. Kitchin, T. Bligaard and H. Jonsson, *The Journal of Physical Chemistry B*, 2004, **108**, 17886-17892.
2. S. Kattel, P. Atanassov and B. Kiefer, *The Journal of Physical Chemistry C*, 2012, **116**, 17378-17383.
3. L. Yu, X. Pan, X. Cao, P. Hu and X. Bao, *Journal of Catalysis*, 2011, **282**, 183-190.
4. S. Zuluaga and S. Stolbov, *The Journal of chemical physics*, 2011, **135**, 134702.